Energy Proceedings
2022
ISSN 2004-2965

Gas engine Oxy Fuel Combustion for Combined Heat and Power Applications

Andrew Cantanhede Cardoso[1], Carlos Alberto Gurgel Veras[2]

1 University of Brasília – Graduate Program in Mechanical Sciences

2 University of Brasília – Energy and Environment Laboratory – University of Brasília – LEA-UnB

ABSTRACT

Oxy-fuel combustion (OFC) is a promising technology for Carbon Capturing and Storage (CCS) in power generation systems. This work presents a mathematical model to predict relevant gas engine parameters for combined heat and power application. Different oxidizer blends (O2 + CO2) for the combustion of refuse-derived fuel pyrolysis gas were tested. Numerical predictions showed that oxy-fuel combustion of RDF pyrolysis gas in power engines did not penalize system thermal efficiency. The exhaust gas temperature and heat content suit combined heat and power plants under zero emissions operation.

Keywords: gas engine, carbon capture and storage, oxy-fuel combustion, waste management, pyrolysis, combined heat and power.

NOMENCLATURE

Abbreviations	
CAC	Conventional Air Combustion
CCS	Carbon Capture and Storage
EGR	Exhaust Gas Recirculation
ICE	Internal Combustion Engine
ICEG	Internal Combustion Engine-Generator
LHV	Lower Heating Value
OFC	Oxy-Fuel Combustion
RDF	Refused-Derived Fuel
SFC	Specific Fuel Consumption
WtE	Waste to Energy
Symbols	
AFR_{mb}	Stoichiometric ratio mass based
AFR_{vb}	Stoichiometric ratio volume based
c_p	Average specific heat capacity of the mix, constant pressure
c_v	Average specific heat capacity of the mix, constant volume
D	Piston bore
h_{in}	Enthalpy of reactants
h_{out}	Enthalpy of products
k_s	Dry friction loss factor
k_w	Wet friction loss factor
$\dot{m}_{oxid}$	Oxidizer mass flow
$\dot{m}_{in}$	Mass input flow
$\dot{m}_{out}$	Mass output flow
$\dot{m}_{eg}$	Exhaust gas flow
N	Cycle strokes
P_e	Engine power
$\bar{p}_c$	Mean compression pressure
$\bar{p}_e$	Mean effective pressure
$\bar{p}_f$	Mean friction pressure
$\bar{p}_{f,0}$	Constant dry friction pressure
$\bar{p}_i$	Mean indicated pressure
r	Charging coefficient
R	Universal gas constant
rpm	Engine speed (cycle per minute)
V_c	Engine total displacement
w	Piston mean velocity
Greek Symbols	
β	Number of CO_2 moles in the oxidizer mix
Δp_r	Pressure difference between exhaust and intake
γ	Number of N_2 moles in the oxidizer mix
$\gamma(T)$	Specific heat ratio
ξ	Convenience factor
ε_E	Engine coefficient losses for exhaust gases
ε_P	Engine coefficient losses for heat transfer to walls (cooling)
ε_R	Engine coefficient losses for air intake
ϕ	Fuel air equivalence ratio
η_e	Engine effective efficiency
η_i	Engine internal efficiency
η_{ind}	Engine indicated efficiency
η_{isc}	Compressor isentropic efficiency
η_{isT}	Turbine isentropic efficiency
η_{mec}	Engine mechanical efficiency
η_{th}	Engine thermal efficiency
ρ_0	Reactants mix density
χ	Compression ratio

This is a paper for the 14th International Conference on Applied Energy - ICAE2022, Aug. 8-11, 2022, Bochum, Germany.

1. INTRODUCTION

Reduction of greenhouse gas emissions claims alternative power generation fuels [1] and advanced burning technologies [2] also avoiding gases that lead to air quality deterioration such as NO_x, carbon monoxide (CO) and hydrocarbons (HC) [3]. The European Union, for instance, has defined ambitious targets for 2030, cutting no less than 40% in greenhouse gas emissions (CO_2, CH_4, N_2O, etc.) from 1990 levels, and improving about 32% overall energy transformation efficiency [4]. Carbon Capture and Storage (CCS) technology combined with more efficient power generation would further reduce CO_2 emissions [5]. Renewable energy sources also play a major role to substitute fossil fuels in any combined strategy to decrease greenhouse gas emissions.

In terms of power generation, Internal Combustion Engines-Generators (ICEGs) play a significant role in developing countries [6] due to their lower cost, larger availability and better fuel flexibility [7] when compared to gas turbines [8]. In Brazil, gas engines have been the preferred technology for landfill gas utilization in WtE projects.

There are few works, however, dealing with oxy-fuel technology in ICE's. This work thus investigates the use of pyrolysis gas from Refuse-Derived Fuels in internal combustion engines running in oxy-fuel mode. Engine operation was modeled to provide relevant data for combined heat and power assessment under oxy-fuel combustion.

2. OXY-FUEL COMBUSTION IN ICE'S

Oxy-fuel combustion relies on using oxygen diluted in recycled carbon dioxide [9] whose combustion process is given by

$$C_xH_yO_z + a(O_2 + \alpha CO_2) \rightarrow bCO_2 + cH_2O \qquad \text{Equation 1.}$$

The CO_2 stoichiometric coefficient (α) may be adjusted for improved system efficiency based on the adopted heat conversion technology. The flue gas is then cooled to condense the water vapor and the captured excess carbon dioxide is stored underground.

According to Rajca et al. [10], gas obtained from RDF pyrolysis has a calorific value in the range of 15-30 MJ/Nm³. The pyrolysis gas is a mixture of varying concentrations of CO, CO_2, CH_4, H_2 and other minor constituents. The fuel is therefore appropriated for OFC technology in terms of energy density and composition.

To perform this goal, a set of equations proposed by Martin [11] were programmed in the Engineering Equation Solver platform [12]. The combined heat and power system is depicted in Fig. 1. Basically, an ICE burns RDF pyrolysis gas under oxy-fuel mode. Oxygen would be provided by a production plant based on cryogenic distillation process, due to its high purity (>95%) and lower cost when compared to pressure swing adsorption [13].

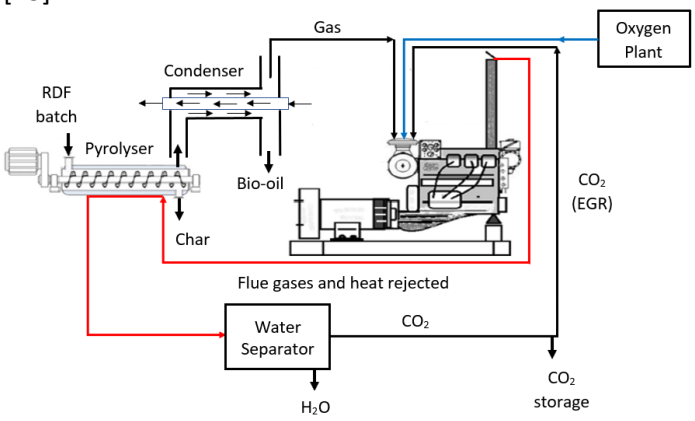

Fig. 1 – CHP plant for oxy-fuel application.

3. METHODOLOGY

3.1 Combustion Engine Modelling

The theory lies on solving a set of thermodynamic equations of a standard four-stroke Otto cycle. The cycle is comprised of an adiabatic irreversible compression (stage 1 to 2), energy addition at near constant volume (stage 2 to 3) irreversible expansion (state 3 to 4), and idealized heat rejection, also at constant volume, to close the cycle (stage 4 to 1). The ideal gas law is used to determine the thermodynamic states.

The model is based on the main processes that take place along the cycle [11]:

$$\eta_{ind} + \varepsilon_P + \varepsilon_E + \varepsilon_R = 1 \qquad \text{Equation 2}$$

In Equation 2, the main processes are given by the indicated engine efficiency from the heat addition (η_{ind}), cooling losses through cylinder walls (ε_P), losses from the exhaust (ε_E), and intake breathing losses (ε_R). Cooling losses depend on the charging coefficient (r), mean piston velocity (w), diameter (D), and the compression ratio (χ):

$$\varepsilon_P = 0.015 \cdot (r \cdot w \cdot D)^{-0,2} \cdot (\chi^{0,8} + 3\,\chi^{-0,4}) \qquad \text{Equation 3}$$

where the charging coefficient is given by

$$r = \left(\eta_{isc}\eta_{isT}\frac{\dot{m}_{eg}h_{inT}}{\dot{m}_{oxid}h_{in_{oxid}}}\right)^{\frac{\gamma(T)}{\gamma(T)-1}}\frac{T_{in_{oxid}}}{T_{out_{oxid}}} \qquad \text{Equation 4}$$

Mixture specific heat capacities, at both constant pressure and constant volume, at any given temperature are calculated with the following equation

$$\gamma(T) = \sum \frac{Y_i c_{p_i}(T)}{Y_i c_{v_i}(T)} \qquad \text{Equation 5}$$

For gaseous fuels, intake breathing losses ε_R are inferred by

$$\varepsilon_R = \frac{\Delta p_R}{r \cdot \rho_0 \cdot \left(\frac{AFR_{vb}}{AFR_{vb}+\phi}\right) \cdot \phi \cdot \frac{LHV}{AFR_{mb}}} \qquad \text{Equation 6}$$

where Δp_R is the difference between exhaust (p_{exh}) and intake (p_{int}) pressures.
Losses from the exhaust are calculated by

$$\varepsilon_E = \frac{1}{\chi^{\xi}} - \varepsilon_P \left(\frac{2}{\chi^{\xi}+1}\right) \qquad \text{Equation 7}$$

where the convenience factor ξ is obtained for the thermodynamic cycle with varying properties, $\gamma = f(T)$,

$$\xi = 0.277 + 0.06(1 - \phi + (1 - 0.1\chi^{0.5})(1 - \phi)^{2,5}) \qquad \text{Equation 8}$$

The overall engine performance can be inferred through a set of equations that are a function of engine sizing, operation regime, fuel type, mechanical friction and mixture compression losses. The losses are established by a set of mean engine pressures. The indicated efficiency in Equation 2 is calculated from the mechanical and effective efficiencies:

$$\eta_e = \eta_{mec}\eta_{ind} \qquad \text{Equation 9}$$

where

$$\eta_{mec} = 1 - \frac{\bar{p}_f}{\bar{p}_i} \qquad \text{Equation 10}$$

In equation 10, average piston friction pressure due to piston rings and lubrication is given by

$$\bar{p}_f = \bar{p}_{f,0} + k_s(2\bar{p}_c + \bar{p}_i)k_w \frac{w}{D} \qquad \text{Equation 11}$$

and mean indicated pressure is inferred with

$$\bar{p}_i = \eta_{ind} r \rho_0 \frac{AFR_{vb}}{(AFR_{vb}+\phi)} \frac{\phi LHV}{AFR_{mb}} \qquad \text{Equation 12}$$

The effective efficiency is calculated from the engine brake power which is a function of the mean effective pressure, engine total displacement, speed, and cycle regime:

$$P_e = \bar{p}_e V_c \frac{rpm}{N} \qquad \text{Equation 13}$$

where

$$\bar{p}_e = \eta_e r \rho_0 \frac{AFR_{vb}}{(AFR_{vb}+\phi)} \frac{\phi LHV}{AFR_{mb}} \qquad \text{Equation 14}$$

The fundamental equations from 2 to 14 were implemented in the EES platform, along with a set of auxiliary equations in order to get relevant engine performance data for combined heat and power applications under CCS technology. A total of 137 equations comprised the model for the oxy-fuel CHP plant.

The presented model was first validated by comparing numerical predictions with performance data of a commercial gas engine (Caterpillar G3520) [14].

For that, it was assumed: $\bar{p}_{f,0} = 70\ kPa$, $k_s = 0{,}02\ kPa$, $k_w = 0{,}70\ kPa$, $\bar{p}_c = 700\ kPa$ for electric generators powered by a gas engine [11].

Validation results and corresponding catalog reference information are presented in Table 1. Similar results were obtained for natural gas and ϕ = 0,57 from the manufacturer's datasheet. As it can be seen, the model is capable of reproducing with a high level of confidence the basic operation of an actual engine. Therefore, relevant data can be obtained for combined heat and power systems assessment.

Table 1 – Code validation.

Parameter	CAC ϕ=0.57	G3520 ϕ=0.57
Thermal efficiency (%)	42.4	45.3
Exhaust gas temperature (°C)	496.4	430
SFC (MJ/kWh)	8.81	8.63
Exhaust heat rejection (kW)	1682	1462
Power output (kW)	2085	2100

4. RESULTS AND DISCUSSION

The model was then applied to simulate different oxidizer compositions (OFC) as presented in table 2 burning RDF pyrolysis. Refuse-Derived Fuel (RDF) pyrolysis gas composition is presented in Table 3 [10].

Table 2 - Oxidizer mixes - Species vol (%)

OFC		CAC	
CO_2	O_2	N_2	O_2
75/80/85	25/20/15	78	21

For fuel and oxidizer compositions used in OFC and CFC simulations, major differences in engine performance are related to the exhaust gas temperature. This was expected due to the larger specific heat of carbon dioxide in comparison to that of nitrogen and the much higher concentration compared to that of water vapor, which has higher specific heat. Exhaust gas temperature and heat rejection for the OFC varies by less than 38% and 8%, respectively. Every 5% increase in CO_2 oxidizer concentration implies a minimum 150 °C drop in exhaust gas temperature while generating an increment

in carbon capture by at least 25% as compared to conventional air combustion.

Table 3 - Fuel composition (RDF) – main species concentration (%)

C_2H_6	C_3H_6	CO_2	H_2	C_2H_4	CH_4	CO
4.3	7.1	11.8	12.4	13.8	17.8	29.6

Table 4 – Numerical predictions for OFC and CAC burning modes.

	OFC 75/25 (ϕ=1)	OFC 80/20 (ϕ=1)	OFC 85/15 (ϕ=1)	CAC (ϕ=1)
CO_2 (exhaust %)	87.2	89.3	91.9	13.5
H_2O (exhaust %)	12.4	9.8	7.4	15.8
N_2 (exhaust %)	0.4	0.9	0.7	70.7
Exhaust mass flow (kg/h)	7542	9430	12578	6529
Exhaust temperature (°C)	846	694.3	530.8	965.3
Heat rejection to exhaust (kW)	2097	2040	1945	2128
Power output (kW)	2217	2200	2172	2223
SFC (MJ/kWh)	8.694	8.76	8.873	8.747
Thermal efficiency (%)	43.01	42.67	42.13	42.74

For the same power input and engine operational conditions, slightly different exhaust gas concentrations of H_2O and CO_2 were obtained by varying the oxidizer composition in OFC mode, as presented in Table 4. Specific fuel consumptions and engine thermal efficiency are also quite similar for all the cases studied, including the conventional combustion process.

According to Rayca et al [10], RDF pyrolysis may take place in the temperature range of 400 °C and 900 °C. The exhaust gas temperatures shown in Table 4 varied from about 530 to 846 °C, when operating in the oxyfuel mode. The amount of heat and the temperature of the flue gases are, therefore, suitable to sustain the pyrolysis reactions inside in combined heat and power operation system. Considering a heat of pyrolysis of about 2500 kJ/kg, the heat rejected by the engine would process near 3000 kg/h of RDF. The CHP plant operating under CCS technology would release almost zero emissions of CO_2. However, a comprehensive cost analysis should be performed to check plant's economic feasibility. A simplified cost analysis is presented in the next section.

5. PRELIMINARY FEASIBILITY ANALYSIS

Brazil operates a large scale state-of-the-art thermoelectric power plant called 'UTE-LORM' comprised of 24 Wärtsilä 20V34SG gas generator sets with a total combined output of 204 MW [15].

Assuming an oxygen plant – coupled to that power plant (204 MW) – with a typical production cost of US$ 0.045/kg for high purity oxygen (>95%) obtained through cryogenic distillation process [13], the study points towards a payback time between 6 and 17 years depending on the OFC operating modes presented in table 4. Cost analysis refer to an oxy-fuel technology implementation on a CHP plant on a 24/7 basis.

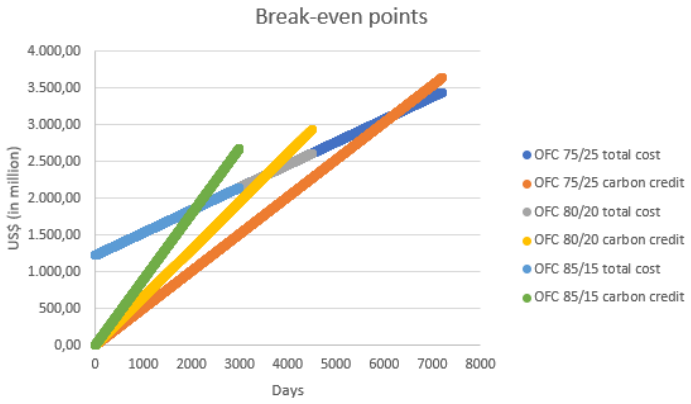

Fig. 2 – Break-even points for different OFC modes for a 204 MW power plant.

This figure was based on a carbon credit of US$ 36/stored CO_2 ton. The authors are elaborating a more detailed feasibility model that will be published in the near future.

6. CONCLUSIONS

A model was developed to estimate relevant gas engine performance parameters under oxy-fuel burning technology for carbon capture and storage of CHP plants.

Numerical predictions showed that oxy-fuel combustion of RDF pyrolysis gas in gas engines did not penalize system thermal efficiency. The exhaust gas temperature and heat content are suitable for combined heat and power plants under zero emissions operation.

A more detailed model for cost analysis should be included in the model for feasibility analysis under the carbon credit approach.

7. REFERENCE

7.1 References

[1] Boloy R, Silveira J, Tuna C, Coronado C, Antunes J. Ecological impacts from syngas burning in internal combustion engine: Technical and Economic aspects. Renewable and Sustainable Energy Reviews. 2011, Vol 15, pp. 5194-5201. DOI: 10.1016/j.rser.2011.04.009

[2] Van Blarigan A, Kozarac D, Seiser R, Cattolica R, Chen J-Y, Dibble R. Experimentaal Study of Methane Fuel Oxycombustion in a Spark Ignited Engine. Journal of Energy Resources Technology. 2013; 136:012203. https://doi.org/10.1115/1.4024974

[3] Serrano J, Arnau F, García-Cuevas L, Farias V. Oxy-fuel combustion feasibility of compression ignition engines using oxygen separation membranes for enabling carbon dioxide capture.

[4] E. Commission, 2030 climate and energy framework in European Union. Accessed on April 2th 2022. URL: https://ec.europa.eu/clima/policies/strategies/2030_en

[5] Xiang Li, Zhijun P, Ajmal T, Aitouche A, Mobasheri R, Pei Y, Gao Bo, Wellers M. A feasibility study of implementation of oxy-fuel combustion on a practical diesel engine at the economical oxygen-fuel ratios by computer simulation. Advances in Mechanical Engineering 2020, Vol 12(12) 1-13. DOI: 10.1177/1687814020980182.

[6] Wärtsilä. Combustion Engine vs Gas Turbine: Fuel Flexibility. Accessed April 12th, 2022. https://www.wartsila.com/energy/learn-more/technical-comparisons/combustion-engine-vs-gas-turbine-fuel-flexibility

[7] Boehman A, Le Corre O. Combustion of Syngas in Internal Combustion Engines. 180:6, 1193-1206, DOI: 10.1080/00102200801963417

[8] Copa J, Tuna C, Silveira J, Boloy R, Brito P, Silva V, Cardoso J, Eusébio D. Techno-Economic Assessment of the Use of Syngas Generated from Biomass to Feed an Internal Combustion Engine. Energies 2020, 13, 3097. DOI: 10.3390/en13123097

[9] Zhihua Wang. Zhihua Wang, 1.23 Energy and Air Pollution, Editor(s): Ibrahim Dincer, Comprehensive Energy Systems, Elsevier, 2018, Pages 909-949, ISBN 9780128149256, https://doi.org/10.1016/B978-0-12-809597-3.00127-9.

[10] Rayca P, Poskart A, Chrubasik M, Sajdak M, Zajemska M, Skibinski A, Korombel A. Technological and economic aspect of Refused Derived Fuel pyrolysis. Renewable Energy, Volume 161, 2020, Pages 482-494, ISSN 0960-1481, https://doi.org/10.1016/j.renene.2020.07.104.

[11] Martin J, Motores de Combustão Interna, Université Catholique de Louvain. UCL. TERM, 2008.

[12] EES,2022. Engineering Equation Solver, F-Chart Software, accessed April 8th, 2022. http://www.fchart.com/ees/

[13] Adhikari B, Orme C, Klaehn J, Stewart F. Technoeconomic analysis of oxygen-nitrogen separation for oxygen enrichment using membranes. Separation and Purification Technology 2021. Volume 268, ISSN 1383-5866, https://doi.org/10.1016/j.seppur.2021.118703.

[14] Caterpillar G3520E. Gas Engine Technical Data. Fuel Flexibility. Accessed April 25th 2022. https://emc.cat.com/pubdirect.ashx?media_string_id=GAS-DM8924-02-GS-EPG-M-13100177.pdf

[15] Wärtsilä. Gas and multi-fuel power plants. Accessed May 20th, 2022 https://cdn.wartsila.com/docs/default-source/power-plants-documents/downloads/brochures/gas-and-multi-fuel-power-plants-2017.pdf